JACS
JOURNAL OF THE AMERICAN CHEMICAL SOCIETY
pubs.acs.org/JACS

Article

Supramolecular Nucleic Acid-Based Organosilica Nanoparticles Responsive to Physical and Biological Inputs

Pierre Picchetti,[▽] Stefano Volpi,[▽] María Sancho-Albero, Marianna Rossetti, Michael D. Dore, Tuan Trinh, Frank Biedermann, Martina Neri, Alessandro Bertucci, Alessandro Porchetta,* Roberto Corradini,* Hanadi Sleiman,* and Luisa De Cola*

Cite This: J. Am. Chem. Soc. 2023, 145, 22903−22912

Read Online

ACCESS | Metrics & More | Article Recommendations | Supporting Information

ABSTRACT: Organosilica nanoparticles that contain responsive organic building blocks as constitutive components of the silica network offer promising opportunities for the development of innovative drug formulations, biomolecule delivery, and diagnostic tools. However, the synthetic challenges required to introduce dynamic and multifunctional building blocks have hindered the realization of biomimicking nanoparticles. In this study, capitalizing on our previous research on responsive nucleic acid-based organosilica nanoparticles, we combine the supramolecular programmability of nucleic acid (NA) interactions with sol−gel chemistry. This approach allows us to create dynamic supramolecular bridging units of nucleic acids in a silica-based scaffold. Two peptide nucleic acid-based monoalkoxysilane derivatives, which self-assemble into a supramolecular bis-alkoxysilane through direct base pairing, were chosen as the noncovalent units inserted into the silica network. In addition, a bridging functional NA aptamer leads to the specific recognition of ATP molecules. In a one-step bottom-up approach, the resulting supramolecular building blocks can be used to prepare responsive organosilica nanoparticles. The supramolecular Watson−Crick−Franklin interactions of the organosilica nanoparticles result in a programmable response to external physical (i.e., temperature) and biological (i.e., DNA and ATP) inputs and thus pave the way for the rational design of multifunctional silica materials with application from drug delivery to theranostics.

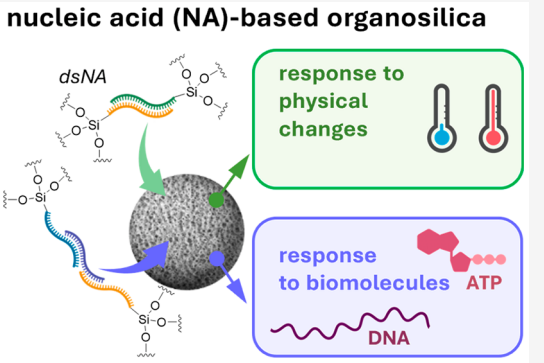

INTRODUCTION

In recent years, the use of nanoparticles (NPs) has led to a number of exciting breakthroughs in medicine, providing new tools for the treatment and detection of diseases.[1−3] Regarding ongoing efforts to endow nanomaterials with the ability to respond to their environment and perform critical tasks for emerging biomedical technologies, the development of supramolecular materials[4,5] and liposomes[6−8] with versatile organic functional structures has shown particular promise. However, creating cost-effective, long-term-stable, and biocompatible NPs that exhibit multifunctionality, such as recognizing disease biomarkers like DNA or small organic molecules and degrading in response to their presence, remains a challenge.[9]

In this regard, using organosilica particles (OSPs)[10] represents a promising strategy for developing smart nanomaterials for biomedical applications. The main advantages of OSPs include their general biocompatibility, tunable physicochemical properties, such as size, shape, and porosity, and the possibility of introducing responsive organic linkers within their framework using well-established sol−gel chemistry.[11] By following such an approach, the organic component is covalently incorporated into a rigid silica framework that can be used in NPs fabrication. The covalent bonds ensure structural stability during the condensation of the silica precursors but limit the possibility of exploiting the dynamic behavior of supramolecular systems (see our work "Responsive Nucleic Acid-Based Organosilica Nanoparticles").[12]

On the other hand, biopolymers such as nucleic acids (NAs) can yield 3D structures with nanometer-precise features and potential applications in biomedical technologies.[13−15] Despite their promising properties, purely synthetic DNA-based materials have several drawbacks, such as lack of *in vivo* stability and challenging large-scale synthesis.[16,17] These have limited, until now, use in real-world nanomedicine applications.[18] Nucleic acids not only self-assemble into double helices and bind to complementary sequences according to programmable Watson−Crick−Franklin base pairing but can also interact with proteins and small molecules through noncovalent interactions. Indeed, several RNA and DNA

Received: May 2, 2023
Published: October 16, 2023

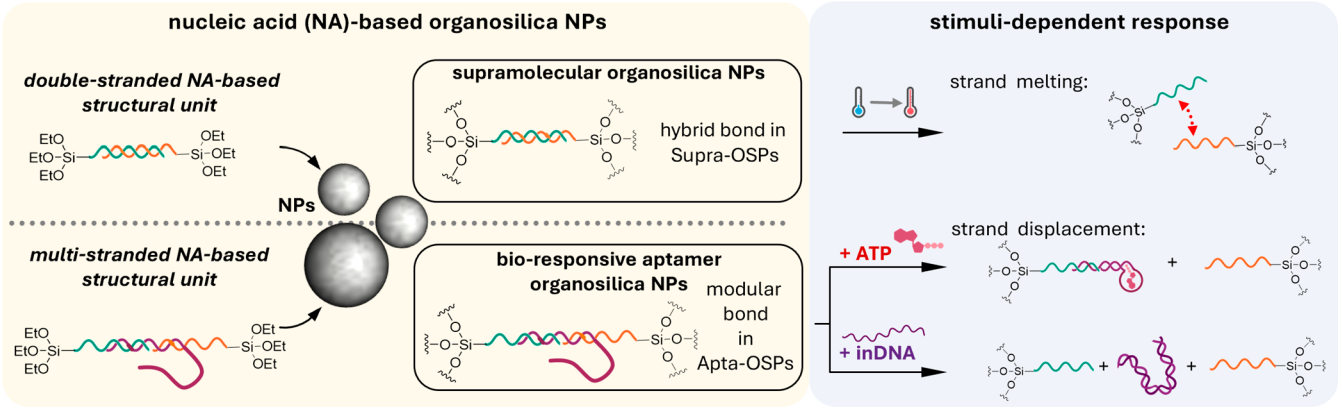

Figure 1. The presence of supramolecular-bridged NA (DNA or PNA) building blocks endows nucleic acid-based organosilicas with sequence-specific chemical, physical, and biological responsiveness.

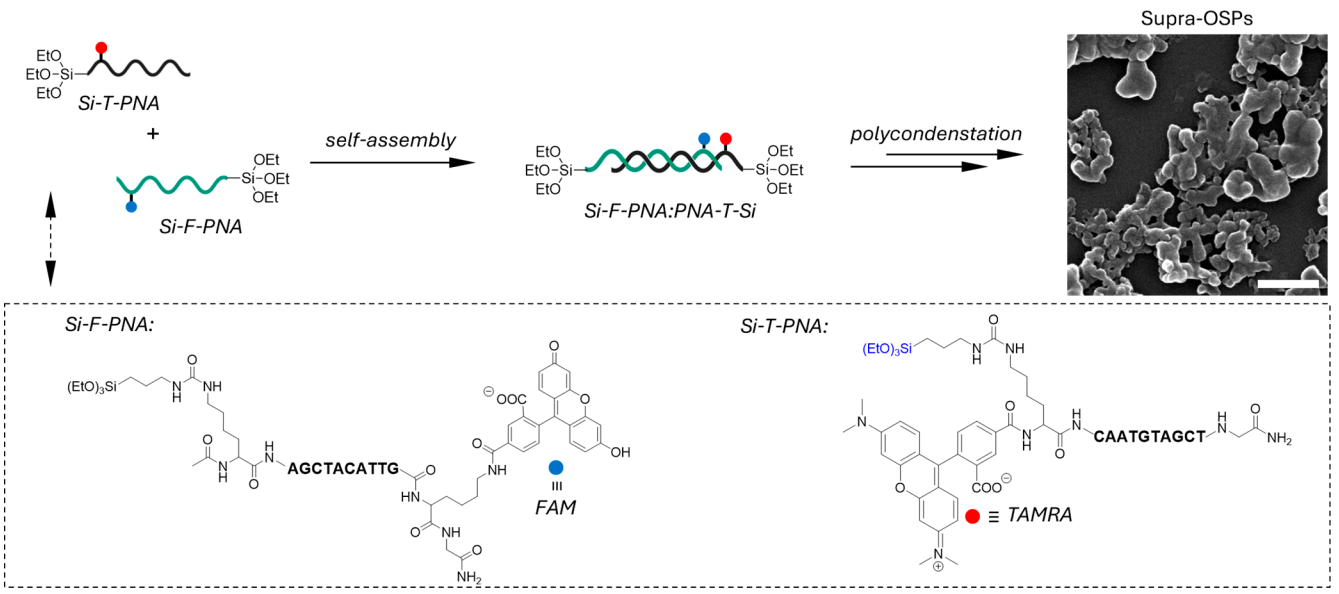

Figure 2. Alkoxysilanes Si-T-PNA and Si-F-PNA self assemble to form a supramolecular bisalkoxysilane, which, after its hydrolysis and polycondensation, yields supra-OSPs as shown in the SEM image (scale bar = 500 nm).

aptamers,[19] a class of synthetic single-stranded oligonucleotides able to recognize and bind to non-nucleic acid targets with high affinity and specificity, have been described in the last decades and developed thanks to SELEX or similar selection strategies.[20−22] DNA aptamers, in particular, have found numerous applications in sensing technologies when used as probes for proteins,[23,24] toxins,[25,26] small organic molecules,[27] or metals[28] and are under development as potential drugs.[29,30] Several protective chemical modifications can be introduced to improve the stability of DNA oligonucleotides, and this can affect their functionality, especially when using aptamers.[31] As an alternative, the use of resistant oligonucleotide analogs, for self-assembly into nanoparticles, has become increasingly important.[17] Peptide nucleic acids (PNAs),[32] polyamide analogs of DNA, are more stable and easier to produce, and their derivatives can be particularly useful in nanotechnology. PNAs have a high affinity and sequence selectivity for DNA and RNA[33] and can form highly stable PNA:DNA:PNA triplexes and PNA:PNA duplexes; high-affinity PNA aptamers were also recently described.[34] In nanofabrication, PNAs are particularly advantageous since they are compatible with both aqueous and organic solvents[35] and, most importantly, are completely resistant to both peptidases and nucleases.[36]

Previous works on merging nucleic acids and silica-based (nano)materials relied on the use of DNA as a purely structural template for the silicification of preformed DNA structures[37,38] and as a tool to load porous particles or functionalize the surface of NPs with nucleic acids for drug delivery[39−42] or sensing applications.[43−45]

Inspired by the unique properties of dynamic self-assembling of biopolymers in nature and capitalizing on the principles of sol−gel chemistry in which organo-alkoxysilanes enable the preparation of self-assembled organic−inorganic hybrid materials[46−51] and responsive organosilica NPs,[52,53] we achieved hybrid nanomaterials that incorporate nucleic acid-based noncovalent bridging units, which can undergo a series of different dynamic processes in the presence of external stimuli.

In our previous work,[12] we demonstrated that organo-alkoxysilane derivatives of NAs can be used to prepare covalently bridged DNA- or PNA-OSPs. Here we extend this concept by creating noncovalent NA-based silica networks using programmed PNA:PNA or PNA:DNA interactions as

https://doi.org/10.1021/jacs.3c04345
J. Am. Chem. Soc. 2023, 145, 22903−22912

constitutive elements. Self-assembled PNA:PNA, PNA:DNA:PNA supramolecular building blocks were used to prepare the OSPs with or without the presence of a secondary silica source (Figure 1). The resulting organosilica nanoparticles contain nucleic acid structures that can respond to physical stimuli (e.g., temperature) and can recognize complementary NA strands or small molecules (e.g., ATP), leading to morphological changes and eventually the disruption of the nanomaterial. To the best of our knowledge, this is the first example of silica-based nanomaterials held together by a network of programmable, stimuli-responsive noncovalent interactions. Our findings highlight exciting possibilities for designing responsive nanoparticles using nontoxic starting materials that can be applied in a broad range of applications, including drug delivery and sensing.

RESULTS AND DISCUSSION

Synthesis of Supramolecular Organosilica Particles. In our previous work,[12] we described the preparation of bis-alkoxysilane oligonucleotides and showed that the resulting biomolecule can be integrated as an active element into mesoporous OSPs. Utilizing the unique complementarity of oligonucleotides mediated by Watson−Crick−Franklin (WCF) base pairing and $\pi-\pi$-stacking interactions, in the current study, we prepared oligonucleotide-based monoalkoxysilane derivatives that can self-assemble into a supramolecular bis-alkoxysilane in a programmable way. The self-assembled bis-alkoxysilane was then used to prepare organosilica particles that have supramolecular and self-assembled organic bridges in their backbones.

For practical reasons, we decided to test this strategy using PNA strands since these bind more strongly than DNA to complementary strands and allow the use of shorter sequences, and then we moved on to a more advanced PNA:DNA-(aptamer)-based example (vide infra).

In the first step, monoalkoxysilane derivatives were prepared from two complementary PNA strands (Supporting Information Section I). One of them was labeled with the carboxyfluorescein dye (FAM), and the other with 5-carboxytetramethylrhodamine (TAMRA), and the resulting derivatives were designated as Si-F-PNA and Si-T-PNA, respectively (Figure 2). This design enabled a FRET-based study of their hybridization (Figure S1).

Mixing equimolar amounts of Si-F-PNA and Si-T-PNA strands led to the formation of the supramolecular Si-F-PNA:PNA-T-Si adduct, which was used to prepare organosilica particles with supramolecular bridging groups (Supra-OSPs) through direct hydrolysis and polycondensation in basic aqueous solutions (Figure 2; Supporting Information Section II.I). The presence of the organic functionalities in the Supra-OSPs was investigated by UV−vis absorption (Figure S2a) and ATR-FTIR spectroscopy (Figure S2b). The amount of PNA incorporated into the Supra-OSPs was analyzed by fluorescence spectroscopy using an emission-based calibration curve of the T-PNA (Figure S3). Fluorescence analysis showed that 95% of the T-PNA and thus also the F-PNA was incorporated into the final particles compared with the original PNA feed, leading to PNA incorporation of 0.02 μmol·mg^{-1} or 6.7% (w/w; Supporting Information Section II.I).

Förster resonance energy transfer (FRET) studies (Figure 3; Supporting Information Section II.II) showed that by heating a dispersion of the particles in water, thermal melting of the PNA:PNA interactions within the Supra-OSPs occurred, as the

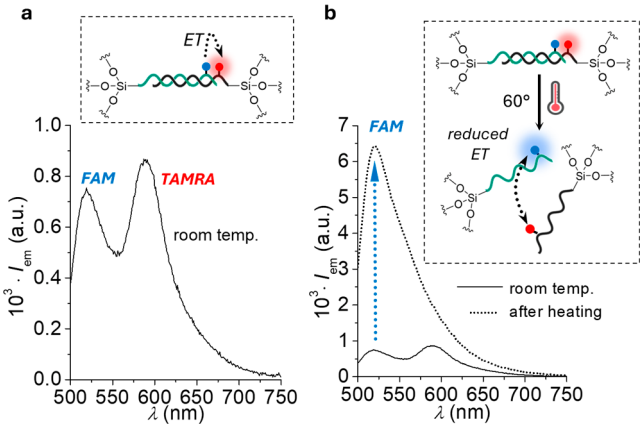

Figure 3. (a) Fluorescence spectra of a dispersion of supra-OSPs (c = 0.008 mg·mL^{-1}) in PBS (pH = 6) at room temperature (λ_{ex} = 450 nm). (b) Overlaid emission spectra of the same supra-OSPs dispersion before and after heating at 60 °C (λ_{ex} = 450 nm).

energy transfer (ET) present in the particles was drastically reduced as well (Figure 3b). Indeed, after heating (T = 60 °C), the emission intensity of fluorescein ($\lambda_{em,FAM}$ = 517 nm) increased by 6-fold and was associated with a negligible change of the TAMRA emission ($\lambda_{em,TAMRA}$ = 590 nm). This result is important because the melting temperature of the PNA:PNA duplex can be easily modulated by changing the length of the PNA double strand, thus enabling fine-tuning of the thermal stability of the NPs. This result can be considered to be a proof of principle for the preparation of supramolecular organosilica particles, opening up possibilities for reversible dynamic systems.

Bioresponsive DNA Aptamer-Bridged Organosilica Particles. Having established that responsive organosilica can be prepared with noncovalent WCF interactions, we used this approach to generate a more complex supramolecular organosilica assembly that can in principle respond to different target biomolecules (bioresponsive aptamer−organosilica NPs in Figure 1) such as complementary DNA or adenosine triphosphate (ATP), the universal energy carrier for living organisms and an essential regulator of cellular processes. We selected an ATP-binding DNA aptamer (Supporting Information Section III.I) since it selectively recognizes ATP through a binding-induced conformational change mechanism.[54,55] As shown in Figure 4a, the ATP aptamer additionally contained a 6-carboxy-X-rhodamine (ROX) label and two PNA-binding regions. These regions were designed to hybridize with two partially complementary PNA silanes: Si-F-PNA (green strand in Figure 4a) and the 8mer Si-PNA8 strand (Figure 4a, orange strand). We confirmed that the modified aptamer used in this work retains its binding affinity to ATP by using ratiometric FRET studies (Supporting Information Section III.III and Figures S4 and S5).

Mixing the aptamer and the two monoalkoxysilane derivatives (Si-F-PNA and Si-PNA8) resulted in a supramolecular bis-alkoxysilane (Si-F-PNA:aptaROX:PNA8-Si; see Figure 4a and Figure S6 for the detailed structure). This supramolecular aggregate was subsequently hydrolyzed and polycondensed in basic aqueous media (pH = 8.5) containing CTAB to yield aptamer-bridged organosilica particles (Apta-OSPs; Supporting Information Section III.IV). The SEM images recorded on Apta-OSPs (Figure 4a right image and Figure S7a) indicated the successful preparation of spherical

https://doi.org/10.1021/jacs.3c04345
J. Am. Chem. Soc. 2023, 145, 22903−22912

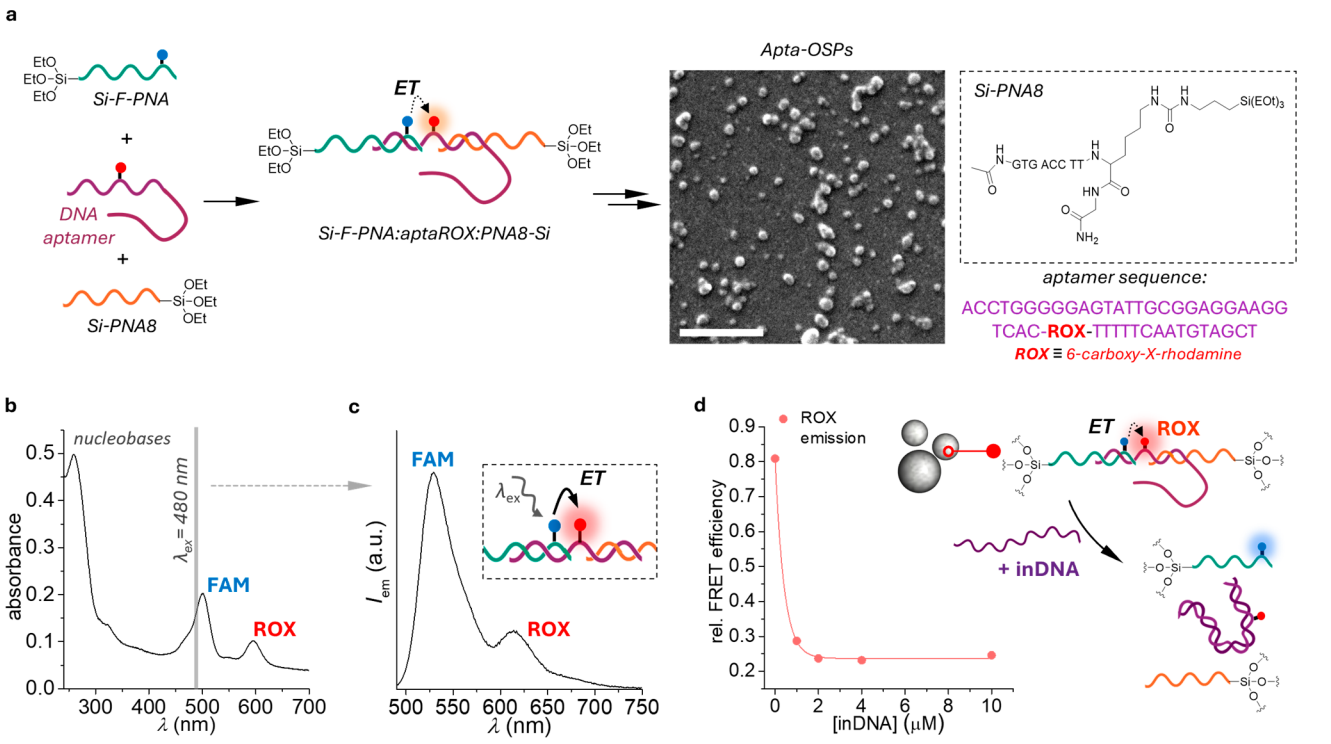

Figure 4. (a) Schematic representation of the self-assembly of two PNA-based monoalkoxysilanes (green and orange strands) that can hybridize with the ATP aptamer to form the supramolecular bis-alkoxysilane derivative (Si-F-PNA:aptaROX:PNA8-Si). The supramolecular alkoxysilane is used to prepare organosilica particles by the hydrolysis and polycondensation of its alkoxysilane groups. On the right, the SEM image of Apta-OSPs is shown (scale bar = 500 nm). (b) UV−vis absorption spectrum of Apta-OSPs ($c_{aptamer}$ = 1.28 μM) in Tris buffer (10 mM, pH 7. 4, with $MgCl_2$, 3 mM). (c) Emission spectrum of Apta-OSPs ($c_{aptamer}$ = 1.28 μM) in Tris buffer (10 mM, pH 7.4, with $MgCl_2$, 3 mM) upon excitation at λ_{ex} = 480 nm. Due to FAM-labeled PNA and ROX-labeled aptamer hybridization, FRET is observed in Apta-OSPs. (d) Schematic representation of the hybridization of the aptamer with DNA, which in turn induces the displacement of the PNA. This process can be followed by decreased sensitized emission of the ROX dye of the aptamer. FRET study on the dispersion of Apta-OSPs (corresponding to 2 μM ROX aptamer) in the presence of different inDNA concentrations (0−10 μM) in Tris-HCl buffer (10 mM, 3 mM $MgCl_2$, pH = 7.4).

nanoparticles with an average diameter of 53 ± 16 nm (Figure S7b).

The synthesis of Apta-OSPs as well as Supra-OSPs was based on a previously reported and optimized procedure for the preparation of DNA-bridged mesoporous organosilica particles.[12] The use of other organoalkoxysilanes and the larger amount of dimethyl sulfoxide likely are the reasons for the differently shaped nanoparticles obtained in this work, as the synthesis of organosilicas is generally strongly dependent on the reaction conditions (e.g., type of organosilanes used, composition of the solvent, temperature, etc.).[11]

The presence of the organic functional groups in the Apta-OSPs was confirmed by ATR-FITR spectroscopy (Figure S8), which revealed a structured but broad transmission band in the range of approximately 3600−3000 cm^{-1} that can be attributed to the N−H and O−H stretching vibrations of the oligonucleotides and to the partially condensed OH groups in the silicate framework of the Apta-OSPs. The sharp transmission bands occurring at 2970, 2910, and 2852 cm^{-1} can be assigned to C_{sp^2}−H and C_{sp^3}−H stretching vibrations originating from the organic components of the particles.[56] The two sharp bands at 1640 and 1560 cm^{-1} reflect the characteristic amide I and II bands, respectively, due to the amide-based backbone of the PNAs.[56] Importantly, the successful condensation of Si-F-PNA:apta:PNA8-Si was confirmed by the emergence of two relatively intense and sharp transmission bands at 1060 and 763 cm^{-1}, reflecting the Si−O−Si stretching vibrations.[57] The presence of some noncondensed Si−OH groups was detected by the appearance of a sharp transmission band at 906 cm^{-1}.[57]

UV−vis spectra were also recorded from a dispersion of Apta-OSPs (Figure 4b) in Tris buffer (10 mM, pH 7.4). These absorbance spectra showed the characteristic absorption band of purine and pyrimidine nucleobases at 260 nm and the band corresponding to the FAM and ROX absorptions with maxima at 500 and 596 nm, respectively, confirming the successful integration of the PNA-aptamer assembly in the Apta-OSPs. The amount of aptamer incorporated into the particles was analyzed by fluorescence spectroscopy using a fluorescence-based calibration curve of the ROX-labeled aptamer (Figure S9). The fluorescence-based analysis showed that 91% of the aptamer was incorporated into the final particles compared with the original aptamer feed, leading to an aptamer incorporation of 0.006 μmol·mg^{-1} or 9% (w/w; Supporting Information Section III.IV).

The integrity of the PNA:aptamer:PNA bridge in Apta-OSPs was verified by FRET spectroscopy. We hypothesized that excitation of the FRET donor (F-PNA) should result in sensitized emission of the FRET acceptor (ROX in the aptamer) due to a distance-dependent ET. As shown in Figure 4c, sensitized ROX emission from the aptamer (λ_{em} = 613 nm) is observed upon excitation of F-PNA (λ_{ex} = 480 nm), confirming that the structural integrity of the aptamer-PNA adduct is preserved after particle formation.

Given the PNA:aptamer:PNA tile design in Apta-OSPs, the responsiveness of Apta-OSPs was explored by challenging the

https://doi.org/10.1021/jacs.3c04345
J. Am. Chem. Soc. 2023, 145, 22903−22912

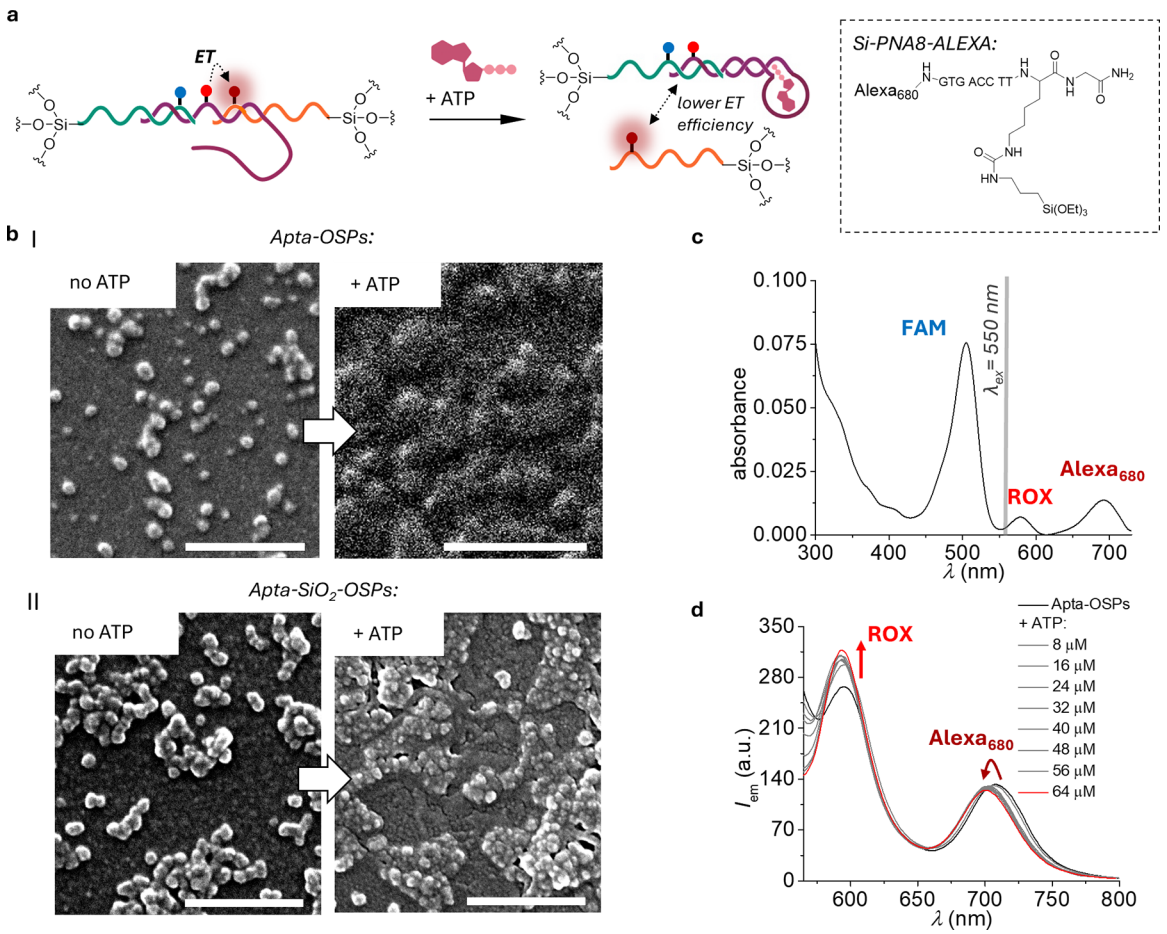

Figure 5. (a) Schematic representation of the strand displacement induced by the presence of ATP within Apta-OSPs. (b) SEM images of (I) Apta-OSPs and (II) Apta-SiO_2-OSPs before and after the addition of ATP (scale bars = 500 nm). The initial spherical morphology of the Apta-OSPs is lost due to displacement of the PNA strand (orange). (c) UV−vis absorption spectra recorded for the dispersion of Apta-OSPs ([Si-F-PNA:aptaROX:PNA8-Si] = 0.012 μM) in Tris buffer (10 mM, pH = 7.4, with $MgCl_2$ = 3 mM). (d) FRET experiments indicated the increase in ROX emission intensities and a concomitant decrease and blue-shifted emission profile of Alexa680 upon addition of ATP to the Apta-OSPs dispersion.

bridging aptamer with a fully complementary invading ssDNA (i.e., inDNA; Supporting Information Section III.II)). Specifically, we hypothesized that the thermodynamically favorable inDNA hybridization with the aptamer due to the presence of extra nucleobases that are not involved in the PNA:aptamer:PNA building block (toehold) would displace the aptamer from the PNAs, thus demonstrating the responsiveness of Apta-OSPs to external DNA molecules and dynamic nature of the supramolecular PNA:aptamer assembly. This process was monitored by FRET analysis using the ROX acceptor-labeled aptamer and donor-containing F-PNA in the NPs. Indeed, mixing Apta-OSPs with increasing concentrations of inDNA resulted in a significant decrease in the relative energy transfer efficiency from the FRET donor to the acceptor, suggesting that toehold-mediated strand displacement occurs (Figure 4d and Supporting Information Section III.V). Thus, this system can recognize and respond to a fully complementary DNA strand, generating a detectable fluorescence response, a finding that may be of interest for imaging and theranostic applications, and targeted release.

The ability of the aptamer to bind ATP once it is integrated as a structural element in Apta-OSPs was similarly investigated by electron microscopy and FRET spectroscopy (Supporting Information Section III.V). The aptamer folding induced by binding to ATP was expected to displace the PNA8 unit (Figure 5a), disrupting the supramolecular bridge in the framework and ultimately triggering degradation and morphological changes in the NPs. As expected, the addition of ATP to a dispersion of Apta-OSPs led to complete particle disintegration, as revealed by SEM microscopy (Figure 5b I). In the case in which Apta-OSPs were prepared by co-condensation of the organic silica precursor TEOS (50 mol % with respect to Si-F-PNA:aptaROX:PNA8-Si and designated herein as Apta-SiO_2-OSPs; Figure S10), particle degradation was still observed upon addition of ATP, although to a lesser extent when compared to Apta-OSPs (Figure 5b II). In this latter case, the formation of morphologically distinct and less spherical particles was observed, as well as an amorphous layer surrounding the particles resulting from a surface reaction with ATP. Importantly, this loss of morphology was observed only in the presence of ATP. Mixing the particles with other biomolecules (e.g., glutathione; GSH) or in water as a control did not cause a drastic morphological change (Figure S11), confirming ATP-triggered strand displacement within Apta-OSPs.

The observed morphological changes can be explained by the structure-switching reconfiguration of the DNA aptamer bound to ATP and the resulting displacement of Si-PNA8

https://doi.org/10.1021/jacs.3c04345
J. Am. Chem. Soc. 2023, 145, 22903−22912

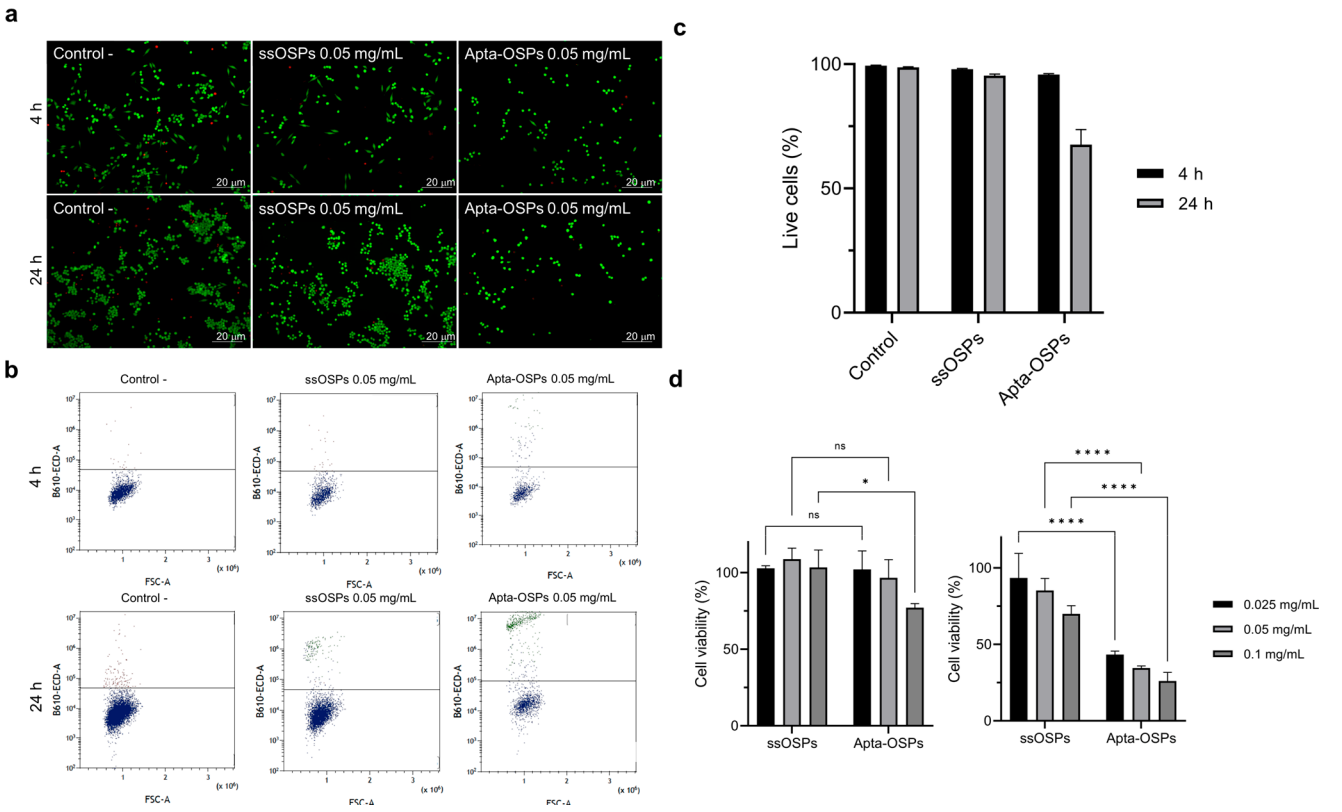

Figure 6. (a) Analysis of live/dead cell viability of 4T1.2 cells treated with ssOSPs and Apta-OSPs (0.05 mg·mL^{-1}) for 4 and 24 h. Images were obtained using FITC and TRITC channels by fluorescence microscopy. Live cells were labeled with calcein-AM (green), and dead cells were colored with EhD-1 (red). (b) Dot plots of propidium iodide flow cytometry analysis of 4T1.2 cells treated with ssOSPs and Apta-OSPs (0.05 mg·mL^{-1}) for 4 and 24 h. (c) Flow cytometry analysis of live/dead cells. (d) MTT assay for cell metabolic activity measurements (left panel, 4 h; right panel, 24 h).

(orange strand) from the supramolecular bridging group. Disruption of the supramolecular bridge leads to pronounced mechanical deformability and structural collapse of the particles.

OSPs which were prepared from 100% Si-F-PNA:aptaR-OX:PNA8-Si showed more drastic morphological changes because they lack additional inorganic silicates, which are structurally robust building blocks that attenuate the effects induced by the ATP binding. The response of Apta-OSPs to the presence of ATP was further confirmed by dynamic light scattering (DLS) analysis, which showed that mixing ATP with the particles triggered their aggregation in an ATP-dependent manner (Figure S12), most likely resulting from the formation of dispersed and fused particle debris, as previously observed in SEM images. In a second control experiment, guanosine 5′-triphosphate (GTP) was added to the Apta-OSPs to follow eventual morphological changes, which in turn would show whether the aptamer retains its selectivity toward ATP. DLS experiments with a dispersion of Apta-OSPs showed that the presence of GTP did not alter their hydrodynamic diameter (Figure S13), indicating the structural integrity of the particles and thus the selectivity of the aptamer for ATP.

To gain further insight into the strand displacement process, we prepared Apta-OSPs with the Alexa680-labeled mono-alkoxy-PNA strand (Si-PNA8-ALEXA; Supporting Information Section I) shown in Figure 5a. This type of fluorescent labeling was used to confirm the dual function of PNA8 as an essential structural component of the supramolecular bridging group in Apta-OSPs and as an ATP-responsive dynamic linker. The absorption spectra of the particles dispersed in Tris buffer (10 mM containing 3 mM $MgCl_2$, pH = 7.4) are depicted in Figure 5c, showing the presence of the three fluorescent dyes in the particles ($\lambda_{ab,max}$ = 500 nm: FAM; $\lambda_{ab,max}$ = 550 nm: ROX; $\lambda_{ab,max}$ = 690 nm: Alexa680). Excitation of the ROX dye ($\lambda_{ex,ROX}$ = 550 nm) resulted in sensitized Alexa680 emission (Figure 5d, black curve), indicating that PNA8-ALEXA is hybridized with the ROX-labeled aptamer in the particles. Conversely, the excitation of PNA8-ALEXA alone at the same wavelength did not result in a significant sensitized emission of the Alexa fluorophore (Figure S14). When ATP was added to the Apta-OSPs dispersion, an increase in the emission intensity of ROX was observed, while the emission intensity of the Alexa680 dye slightly decreased and its emission spectrum exhibited a hypsochromic shift (Figure 5d; Supporting Information Section III.V). These observed photophysical changes showed that the aptamer binds to ATP, displacing the Alexa680-labeled PNA-8 strand, resulting in decreased efficiency of energy transfer from the excited state of the donor dye (ROX) to the acceptor dye (ALEXA). The FRET-based experiment, in combination with the previously described electron microscopy analysis, showed that the aptamer remained accessible and functional after particle formation and that a visible change in particle morphology was observed in the presence of ATP due to the dynamic displacement process within the supramolecular bridging group of Apta-OSPs. From the studies presented here, it appears that ATP recognition by Apta-OSPs begins at the surface of the particles. In this scenario, most aptamer

https://doi.org/10.1021/jacs.3c04345
J. Am. Chem. Soc. 2023, 145, 22903−22912

molecules remain unaffected by the addition of ATP and thus "dormant" until the surface of Apta-OSPs is degraded, allowing new ATP molecules to diffuse to newly available aptamer sites. In addition, the limited accessibility of aptamers in the inner particle scaffold explains why significant photophysical and morphological changes were observed in the presence of an excess of ATP when compared to the amount of aptamer used for the preparation of Apta-OSPs.

Apta-OSPs' Intracellular Entry and Metabolic Activity. The internalization of Apta-OSPs into breast cancer 4T1.2 cells was assessed by confocal microscopy (see Supporting Information Section IV). After the 4T1.2 cells were treated with Apta-OSPs (0.05 mg·mL^{-1}) under standard cell culture conditions, they were fixed and labeled with WGA-Alexa488 (cell membrane) and Hoechst 33342 (nuclei). Apta-OSPs particles were imaged upon excitation at 561 nm (ROX labeled). Representative images from 4T1.2 cells after treatment with Apta-OSPs for 4 and 24 h are shown in Figure S15 and Video S1. The analysis of the red fluorescent signal and the Z-stack sections of the images confirmed the intracellular localization of the Apta-OSPs at the shortest time point (4 h). The punctate emission observed for Apta-OSPs is consistent with an endosomal uptake pathway that we have also previously observed and studied in detail for other organosilica nanoparticles.[58]

After the demonstration that Apta-OSPs were successfully localized in the cell, a live/dead test was carried out to evaluate the viability of Apta-OSP-treated cells. In this assay, ethidium homodimer-1 (EthD-1) is employed for labeling damaged membranes. EthD-1 is excluded by the intact plasma membrane of live cells, and the determination of cell viability depends only on these physical properties. Disulfide-bridged mesoporous organosilica NPs (ssOSPs) were also tested as a control (see Supporting Information Section IV, Figure S22). The live/dead results (live green cells were labeled with calcein-AM and dead cells are shown in red after the incubation with EthD-1, Figure 6a) show that almost 100% of the cells were alive after the treatment with ssOSPs and Apta-OSPs (0.05 mg·mL^{-1}) for 4 h. After 24 h of incubation, untreated and ssOSP-treated cells continued their replication, and the number of living cells significantly increased. In contrast, Asp-OSP-treated cells decrease their level of replication and proliferation. Very similar results were observed by flow cytometry (Figure 6b,c). 4T1.2 cells treated with ssOSPs exhibited high cell viability levels (around 100%), similar to control (untreated) cells after incubation for 4 and 24 h. On the contrary, for the highest time point (24 h), a decrease in cell viability for the Asp-OSP-treated cells was clearly observed (67% of the cells were alive).

To assess whether the decrease in cell viability and the reduction in cell proliferation were related to a reduction in intracellular metabolic activity (caused by the internalization of Apta-OSPs), an MTT metabolic study was performed (Figure 6d). The MTT assay provides information about the intracellular redox balance and the mitochondrial dehydrogenases in living cells.[59] This metabolic activity is strongly influenced by the ATP concentration. After 4 and 24 h of exposure, no significant effects on cell viability were observed for the ssOSPs. However, cells treated with Apta-OSPs exhibited a decrease in metabolic activity and, as a result, cell viability. This decrease was statistically significant for the highest dose (0.1 mg·mL^{-1}) at the lowest incubation time point (4 h). After 24 h of incubation, 4T1.2 cells exhibited a significant decrease in cellular activity, even at the lowest doses. This observation suggests that this effect may be related to the disruption of intracellular ATP metabolism by Apta-OSPs as well as to a silencing activity of the internalized aptamer and PNAs.[59−62]

CONCLUSIONS

This work shows that nucleic acid-derived alkoxysilanes held together by supramolecular interactions can be used for a one-step, bottom-up synthesis of functional organosilica NPs responsive to physical and biochemical inputs. From a materials chemistry point of view, the presence of Watson−Crick−Franklin interactions leads to dynamic and programmable behavior that can be explored for various applications. We showed that introducing dsPNA bridging groups as structural units in organosilica NPs made the noncovalent self-assembling organo-alkoxysilanes temperature-sensitive. Additionally, using a three-component tile-type design, we extended the supramolecular approach and introduced an ATP-responsive DNA aptamer in the structural framework of organosilica NPs. This system turned out to be versatile, since the DNA aptamer is sensitive to both complementary oligonucleotides and to its target ATP molecule with different mechanisms based on noncovalent interactions, which can be monitored via fluorescence spectroscopy. Disruption of the morphology by ATP was confirmed by electron microscopy imaging. Cell uptake experiments also show that Apta-OSPs are readily taken up by breast cancer cells and alter their metabolic activity. We envisage that the preparation of organosilica nanoparticles as presented herein will enhance the ability to develop responsive materials that could possibly be exploited for the targeted delivery of drugs and bioactive molecules, nanoparticle-based gene therapy, and the preparation of nanoparticle-based methods for the detection of oligonucleotides, biomolecules, or even toxins in biofluids and wastewaters.

ASSOCIATED CONTENT

Supporting Information

The Supporting Information is available free of charge at https://pubs.acs.org/doi/10.1021/jacs.3c04345.

Details about instruments, materials, methods, supporting figures, and chemical synthesis (PDF)

3D projection of a Z stack of confocal microscopic images of cells incubated with Apta-OSPs (at 4 h) (MP4)

AUTHOR INFORMATION

Corresponding Authors

Alessandro Porchetta − *Department of Chemistry, University of Rome, Rome 00133, Italy;* orcid.org/0000-0002-4061-5574; Email: alessandro.porchetta@uniroma2.it

Roberto Corradini − *Department of Chemistry, Life Sciences and Environmental Sustainability, University of Parma, 43124 Parma, Italy;* orcid.org/0000-0002-8026-0923; Email: roberto.corradini@unipr.it

Hanadi Sleiman − *Department of Chemistry, McGill University, Montreal, Québec City H3A 0B8, Canada;* orcid.org/0000-0002-5100-0532; Email: hanadi.sleiman@mcgill.com

Luisa De Cola − *Karlsruhe Institute of Technology (KIT), Institute of Nanotechnology (INT), Eggenstein-Leopoldshafen*

76344, Germany; Department of Molecular Biochemistry and Pharmacology, Instituto di Ricerche Farmacologiche Mario Negri, IRCCS, 20156 Milano, Italy; Dipartimento DISFARM, University of Milano, 20133 Milano, Italy; orcid.org/0000-0002-2152-6517; Email: luisa.decola@marionegri.it

Authors

Pierre Picchetti − *Karlsruhe Institute of Technology (KIT), Institute of Nanotechnology (INT), Eggenstein-Leopoldshafen 76344, Germany;* orcid.org/0000-0002-0689-5998

Stefano Volpi − *Department of Chemistry, Life Sciences and Environmental Sustainability, University of Parma, 43124 Parma, Italy*

María Sancho-Albero − *Department of Molecular Biochemistry and Pharmacology, Instituto di Ricerche Farmacologiche Mario Negri, IRCCS, 20156 Milano, Italy*

Marianna Rossetti − *Department of Chemistry, University of Rome, Rome 00133, Italy*

Michael D. Dore − *Department of Chemistry, McGill University, Montreal, Québec City H3A 0B8, Canada;* Present Address: M.D.D.: Department of Chemistry, Northwestern University, Evanston, Illinois 60208, United States; orcid.org/0000-0002-9721-3189

Tuan Trinh − *Department of Chemistry, McGill University, Montreal, Québec City H3A 0B8, Canada;* Present Address: T.T.: Department of Radiology, Stanford University, Stanford, California 94305, United States; orcid.org/0000-0002-0074-9746

Frank Biedermann − *Karlsruhe Institute of Technology (KIT), Institute of Nanotechnology (INT), Eggenstein-Leopoldshafen 76344, Germany;* orcid.org/0000-0002-1077-6529

Martina Neri − *Department of Chemistry, Life Sciences and Environmental Sustainability, University of Parma, 43124 Parma, Italy;* orcid.org/0000-0002-2039-9026

Alessandro Bertucci − *Department of Chemistry, Life Sciences and Environmental Sustainability, University of Parma, 43124 Parma, Italy;* orcid.org/0000-0003-4842-9909

Complete contact information is available at: https://pubs.acs.org/10.1021/jacs.3c04345

Author Contributions

[▽]P.P. and S.V. contributed equally to this work.

Notes

The authors declare no competing financial interest.

■ ACKNOWLEDGMENTS

The authors acknowledge the financial support from the European Union's Horizon 2020 Research and Innovation Program under the Marie Skłodowska-Curie grant agreement "Nano-Oligo Med" (no. 778133). This work has also benefited from the infrastructure and framework of the COMP-HUB Initiative, funded by the Departments of Excellence program of the Italian Ministry for Education, University, and Research (MIUR, 2018-2022). M.S.-A. was supported by an AIRC Fellowship for Italy. We thank Dr. Victor Sebastian of the University of Zaragoza and LMA for the TEM images of ssOSPs.

■ ABBREVIATIONS

ATR, attenuated total reflectance; ATP, adenosine triphosphate; Apta-OSPs, aptamer-bridged organosilica particles; CTAB, cetyltrimethylammonium bromide; DLS, dynamic light scattering; EthD-1, ethidium homodimer-1; FAM, carboxyfluorescein; FRET, Förster resonance energy transfer; FTIR, Fourier transform infrared spectroscopy; GTP, guanosine-5′-triphosphate; ICPTES, 3-(triethoxysilyl)propyl isocyanate; MTT, 3-(4,5-dimethylthiazol-2-yl)-2,5-diphenyltetrazolium bromide; NAs, nucleic acids; NPs, nanoparticles; OSPs, organosilica particles; PNA, peptide nucleic acid; ROX, 6-carboxy-X-rhodamine; ssDNA, single-stranded DNA; ssOSPs, disulfide-bridged mesoporous organosilica particles; TAMRA, 5-carboxytetramethylrhodamine; TEM, transmission electron microscopy; TEOS, tetraethyl orthosilicate; WCF, Watson−Crick−Franklin

■ REFERENCES

(1) Mitchell, M. J.; Billingsley, M. M.; Haley, R. M.; Wechsler, M. E.; Peppas, N. A.; Langer, R. Engineering precision nanoparticles for drug delivery. *Nat. Rev. Drug. Discovery* **2021**, *20*, 101−124.

(2) Ehlerding, E. B.; Grodzinski, P.; Cai, W.; Liu, C. H. Big Potential from Small Agents: Nanoparticles for Imaging-Based Companion Diagnostics. *ACS Nano* **2018**, *12*, 2106−2121.

(3) Kim, B. Y. S.; Rutka, J. T.; Chan, W. C. W. Nanomedicine. *N. Engl. J.* **2010**, *363*, 2434−2443.

(4) Álvarez, Z.; Kolberg-Edelbrock, A. N.; Sasselli, I. R.; Ortega, J. A.; Qiu, R.; Syrgiannis, Z.; Mirau, P. A.; Chen, F.; Chin, S. M.; Weigand, S.; Kiskinis, E.; Stupp, S. I. Bioactive scaffolds with enhanced supramolecular motion promote recovery from spinal cord injury. *Science* **2021**, *374*, 848−856.

(5) Dong, R.; Zhou, Y.; Huang, X.; Zhu, X.; Lu, Y.; Shen, J. Functional supramolecular polymers for biomedical applications. *Adv. Mater.* **2015**, *27*, 498−526.

(6) Dane, E. L.; Belessiotis-Richards, A.; Backlund, C.; Wang, J.; Hidaka, K.; Milling, L. E.; Bhagchandani, S.; Melo, M. B.; Wu, S.; Li, N.; Donahue, N.; Ni, K.; Ma, L.; Okaniwa, M.; Stevens, M. M.; Alexander-Katz, A.; Irvine, D. J. STING agonist delivery by tumour-penetrating PEG-lipid nanodiscs primes robust anticancer immunity. *Nat. Mater.* **2022**, *21*, 710−720.

(7) Liu, S.; Cheng, Q.; Wei, T.; Yu, X.; Johnson, L. T.; Farbiak, L.; Siegwart, D. J. Membrane-destabilizing ionizable phospholipids for organ-selective mRNA delivery and CRISPR-Cas gene editing. *Nat. Mater.* **2021**, *20*, 701−710.

(8) Allen, T. M.; Cullis, P. R. Liposomal drug delivery systems: from concept to clinical applications. *Adv. Drug. Delivery Rev.* **2013**, *65*, 36−48.

(9) Blum, A. P.; Kammeyer, J. K.; Rush, A. M.; Callmann, C. E.; Hahn, M. E.; Gianneschi, N. C. Stimuli-Responsive Nanomaterials for Biomedical Applications. *J. Am. Chem. Soc.* **2015**, *137*, 2140−2154.

(10) Inagaki, S.; Guan, S.; Ohsuna, T.; Terasaki, O. An ordered mesoporous organosilica hybrid material with a crystal-like wall structure. *Nature* **2002**, *416*, 304−307.

(11) Croissant, J. G.; Fatieiev, Y.; Almalik, A.; Khashab, N. M. Mesoporous Silica and Organosilica Nanoparticles: Physical Chemistry, Biosafety, Delivery Strategies, and Biomedical Applications. *Adv. Healthc. Mater.* **2018**, *7*, 1700831.

(12) Picchetti, P.; Volpi, S.; Rossetti, M.; Dore, M. D.; Trinh, T.; Biedermann, F.; Neri, M.; Bertucci, A.; Porchetta, A.; Corradini, R.; Sleiman, H.; De Cola, L. Responsive Nucleic Acid-Based Organosilica Nanoparticles. *J. Am. Chem. Soc.* **2023**, DOI: 10.1021/jacs.3c00393.

(13) Jiang, Q.; Song, C.; Nangreave, J.; Liu, X.; Lin, L.; Qiu, D.; Wang, Z. G.; Zou, G.; Liang, X.; Yan, H.; Ding, B. DNA Origami as a Carrier for Circumvention of Drug Resistance. *J. Am. Chem. Soc.* **2012**, *134*, 13396−13403.

(14) Hu, Q.; Li, H.; Wang, L.; Gu, H.; Fan, C. DNA Nanotechnology-Enabled Drug Delivery Systems. *Chem. Rev.* **2019**, *119*, 6459−6506.
(15) Seeman, N. C.; Sleiman, H. F. DNA Nanotechnology. *Nat. Rev. Mater.* **2018**, *3*, 17068.
(16) Lacroix, A.; Sleiman, H. F. DNA Nanostructures: Current Challenges and Opportunities for Cellular Delivery. *ACS Nano* **2021**, *15*, 3631−3645.
(17) Chandrasekaran, A. R. Nuclease Resistance of DNA Nanostructures. *Nat. Rev. Chem.* **2021**, *5*, 225−239.
(18) Ferguson, B. S.; Hoggarth, D. A.; Maliniak, D.; Ploense, K.; White, R. J.; Woodward, N.; Hsieh, K.; Bonham, A. J.; Eisenstein, M.; Kippin, T. E.; Plaxco, K. W. Real-time, aptamer-based tracking of circulating therapeutic agents in living animals. *Sci. Transl. Med.* **2013**, *5*, 213ra165.
(19) Li, L.; Xu, S.; Yan, H.; Li, X.; Yazd, H. S.; Li, X.; Huang, T.; Cui, C.; Jiang, J.; Tan, W. Nucleic Acid Aptamers for Molecular Diagnostics and Therapeutics: Advances and Perspectives. *Angew. Chem., Int. Ed.* **2021**, *60*, 2221−2231.
(20) Ellington, A. D.; Szostak, J. W. *In vitro* selection of RNA molecules that bind specific ligands. *Nature* **1990**, *346*, 818−822.
(21) Blind, M.; Blank, M. Aptamer Selection Technology and Recent Advances. *Mol. Ther. Nucleic Acids.* **2015**, *4*, e223.
(22) Kong, D.; Yeung, W.; Hili, R. In Vitro Selection of Diversely Functionalized Aptamers. *J. Am. Chem. Soc.* **2017**, *139*, 13977−13980.
(23) Kim, Y. S.; Raston, N. H. A.; Gu, M. B. Aptamer-based nanobiosensors. *Biosens. Bioelectron.* **2016**, *76*, 2−19.
(24) Jo, H.; Gu, H.; Jeon, W.; Youn, H.; Her, J.; Kim, S.-K.; Lee, J.; Shin, J. H.; Ban, C. Electrochemical Aptasensor of Cardiac Troponin I for the Early Diagnosis of Acute Myocardial Infarction. *Anal. Chem.* **2015**, *87*, 9869−9875.
(25) Shim, W. B.; Kim, M. J.; Mun, H.; Kim, M. G. An aptamer-based dipstick assay for the rapid and simple detection of aflatoxin B1. *Biosens. Bioelectron.* **2014**, *62*, 288−294.
(26) Bianco, M.; Sonato, A.; De Girolamo, A.; Pascale, M.; Romanato, F.; Rinaldi, R.; Arima, V. An aptamer-based SPR-polarization platform for high sensitive OTA detection. *Sens. Actuators B* **2017**, *241*, 314−320.
(27) Nakatsuka, N.; Yang, K.-A.; Abendroth, J. M.; Cheung, K. M.; Xu, X.; Yan, H.; Zhao, C.; Zhu, B.; Rim, Y. S.; Yang, Y.; Weiss, P. S.; Stonjanovic, M. N.; Andrews, A. M. Aptamer-field-effect transistors overcome Debye length limitations for small-molecule sensing. *Science* **2018**, *362*, 319−324.
(28) Guo, W.; Zhang, C.; Ma, T.; Liu, X.; Chen, Z.; Li, S.; Deng, Y. Advances in aptamer screening and aptasensors' detection of heavy metal ions. *J. Nanobiotechnology* **2021**, *19*, 166.
(29) Yuhan, J.; Zhu, L.; Zhu, L.; Huang, K.; He, X.; Xu, W. Cell-specific aptamers as potential drugs in therapeutic applications: A review of current progress. *J. Contr. Rel.* **2022**, *346*, 405−420.
(30) Zhu, G.; Chen, X. Aptamer-based targeted therapy. *Adv. Drug Delivery Rev.* **2018**, *134*, 65−78.
(31) Darfeuille, F.; Hansen, J. B.; Orum, H.; Di Primo, C.; Toulmé, J.-J. LNA/DNA chimeric oligomers mimic RNA aptamers targeted to the TAR RNA element of HIV-1. *Nucleic Acids Res.* **2004**, *32*, 3101−3107.
(32) Egholm, M.; Buchardt, O.; Nielsen, P. E.; Berg, R. H. Peptide Nucleic Acids (PNA). Oligonucleotide Analogues with an Achiral Peptide Backbone. *J. Am. Chem. Soc.* **1992**, *114*, 1895−1897.
(33) Saarbach, J.; Sabale, P. M.; Winssinger, N. Peptide nucleic acid (PNA) and its applications in chemical biology, diagnostics, and therapeutics. *Curr. Opin. Chem. Biol.* **2019**, *52*, 112−124.
(34) Rodrigues, T.; Curti, F.; Leroux, Y. R.; Barras, A.; Pagneux, Q.; Happy, H.; Kleber, C.; Boukherroub, R.; Hasler, R.; Volpi, S.; Careri, M.; Corradini, R.; Szunerits, S.; Knoll, W. Discovery of a Peptide Nucleic Acid (PNA) aptamer for cardiac troponin I: Substituting DNA with neutral PNA maintains picomolar affinity and improves performances for electronic sensing with graphene field-effect transistors (gFET). *Nano Today* **2023**, *50*, 101840.
(35) Sen, A.; Nielsen, P. E. On the stability of peptide nucleic acid duplexes in the presence of organic solvents. *Nucleic Acids Res.* **2007**, *35*, 3367−3374.
(36) Demidov, V. V.; Potman, V. N.; Frank-Kamenetskii, M. D.; Egholm, M.; Buchard, O.; Sönnichsen, S. H.; Nielsen, P. E. Stability of peptide nucleic acids in human serum and cellular extracts. *Biochem. Pharmacol.* **1994**, *48*, 1310−1313.
(37) Liu, X.; Zhang, F.; Jing, X.; Pan, M.; Liu, P.; Li, W.; Zhu, B.; Li, J.; Chen, H.; Wang, L.; Lin, J.; Liu, Y.; Zhao, D.; Yan, H.; Fan, C. Complex silica composite nanomaterials templated with DNA origami. *Nature* **2018**, *559*, 593−598.
(38) Nguyen, L.; Doblinger, M.; Liedl, T.; Heuer-Jungemann, A. DNA-Origami-Templated Silica Growth by Sol-Gel Chemistry. *Angew. Chem., Int. Ed.* **2019**, *58*, 912−916.
(39) Lülf, H.; Bertucci, A.; Septiadi, D.; Corradini, R.; De Cola, L. Multifunctional Inorganic Nanocontainers for DNA and Drug Delivery into Living Cells. *Eur. J. Chem.* **2014**, *20*, 10900−10904.
(40) Dhar, S.; Gu, F. X.; Langer, R.; Farokhzad, O. C.; Lippard, S. J. Targeted delivery of cisplatin to prostate cancer cells by aptamer functionalized Pt(IV) prodrug-PLGA-PEG nanoparticles. *Proc. Natl. Acad. Sci. U. S. A.* **2008**, *105*, 17356−17361.
(41) Kim, B.; Sun, S.; Varner, J. A.; Howell, S. B.; Ruoslahti, E.; Sailor, M. J. Securing the Payload, Finding the Cell, and Avoiding the Endosome: Peptide-Targeted, Fusogenic Porous Silicon Nanoparticles for Delivery of siRNA. *Adv. Mater.* **2019**, *31*, 1902952.
(42) Xia, T.; Kovochich, M.; Liong, M.; Meng, H.; Kabehie, S.; George, S.; Zink, J. I.; Nel, A. E. Polyethyleneimine Coating Enhances the Cellular Uptake of Mesoporous Silica Nanoparticles and Allows Safe Delivery of siRNA and DNA Constructs. *ACS Nano* **2009**, *3*, 3273−3286.
(43) Pavlov, V.; Xiao, Y.; Shlyahovsky, B.; Willner, I. Aptamer-Functionalized Au Nanoparticles for the Amplified Optical Detection of Thrombin. *J. Am. Chem. Soc.* **2004**, *126*, 11768−11769.
(44) Song, Y.; Shi, Y.; Huang, M.; Wang, W.; Wang, Y.; Cheng, J.; Lei, Z.; Zhu, Z.; Yang, C. Bioinspired Engineering of a Multivalent Aptamer-Functionalized Nanointerface to Enhance the Capture and Release of Circulating Tumor Cells. *Angew. Chem., Int. Ed.* **2019**, *58*, 2236−2240.
(45) Cutler, J. I.; Auyeung, E.; Mirkin, C. A. Spherical nucleic acids. *J. Am. Chem. Soc.* **2012**, *134*, 1376−1391.
(46) Shimizu, I.; Okabayashi, H.; Hattori, N.; Taga, K.; Yoshino, A.; O'Connor, C. J. 13C-and 1H-NMR and FTIR spectroscopic evidence for aggregate formation of organosilanes in toluene. *Colloid Polym. Sci.* **1997**, *275*, 293−297.
(47) Dieudonne, P.; Man, M. W.; Pichon, B. P.; Vellutini, L.; Bantignies, J. L.; Blanc, C.; Creff, G.; Finet, S.; Sauvajol, J. L.; Bied, C.; Moreau, J. J. In situ X-ray Measurements to Probe a New Solid-State Polycondensation Mechanism for the Design of Supramolecular Organo-Bridged Silsesquioxanes. *Small* **2009**, *5*, 503−510.
(48) Parikh, A. N.; Schivley, M. A.; Koo, E.; Seshadri, K.; Aurentz, D.; Mueller, K.; Allara, D. L. n-Alkylsiloxanes: From Single Monolayers to Layered Crystals. The Formation of Crystalline Polymers from the Hydrolysis of n-Octadecyltrichlorosilane. *J. Am. Chem. Soc.* **1997**, *119*, 3135−3143.
(49) Mouawia, R.; Mehdi, A.; Rey, C.; Corriu, R. Direct synthesis of ordered and highly functionalized organosilicas containing carboxylic acid groups. *J. Mater. Chem.* **2007**, *17*, 616−618.
(50) Ni, L.; Chemtob, A.; Croutxé-Barghorn, C.; Brendlé, J.; Vidal, L.; Rigolet, S. Kinetics, Thermodynamics, and Dynamics in Organosilane Self-Assembly. *J. Phys. Chem. C* **2012**, *116*, 24320−24330.
(51) Barboiu, M.; Cerneaux, S.; van der Lee, A.; Vaughan, G. Ion-Driven ATP Pump by Self-Organized Hybrid Membrane Materials. *J. Am. Chem. Soc.* **2004**, *126*, 3545−3550.
(52) Quignard, S.; Masse, S.; Laurent, G.; Coradin, T. Introduction of disulfide bridges within silica nanoparticles to control their intracellular degradation. *Chem. Commun.* **2013**, *49*, 3410−3412.
(53) Talamini, L.; Picchetti, P.; Ferreira, L. M.; Sitia, G.; Russo, L.; Violatto, M. B.; Travaglini, L.; Fernandez Alarcon, J.; Righelli, L.;

https://doi.org/10.1021/jacs.3c04345
J. Am. Chem. Soc. 2023, 145, 22903−22912

Bigini, P.; De Cola, L. Organosilica Cages Target Hepatic Sinusoidal Endothelial Cells Avoiding Macrophage Filtering. *ACS Nano* **2021**, *15*, 9701−9716.
(54) Del Grosso, E.; Ragazzon, G.; Prins, L. J.; Ricci, F. Fuel-Responsive Allosteric DNA-Based Aptamers for the Transient Release of ATP and Cocaine. *Angew. Chem., Int. Ed.* **2019**, *58*, 5582−5586.
(55) Del Grosso, E.; Idili, A.; Porchetta, A.; Ricci, F. A modular clamp-like mechanism to regulate the activity of nucleic-acid target-responsive nanoswitches with external activators. *Nanoscale* **2016**, *8*, 18057−18061.
(56) Mateo-Martí, E.; Briones, C.; Román, E.; Briand, E.; Pradier, C. M.; Martín-Gago, J. A. Self-Assembled Monolayers of Peptide Nucleic Acids on Gold Surfaces: A Spectroscopic Study. *Langmuir* **2005**, *21*, 9510−9517.
(57) Aguiar, H.; Serra, J.; González, P.; León, B. Structural study of sol-gel silicate glasses by IR and Raman spectroscopies. *J. Non. Cryst. Solids* **2009**, *355*, 475−480.
(58) Sancho-Albero, M.; Facchetti, G.; Panini, N.; Meroni, M.; Bello, E.; Rimoldi, I.; Zucchetti, M.; Frapolli, R.; De Cola, L. Enhancing Pt(IV) Complexes' Anticancer Activity upon Encapsulation in Stimuli-Responsive Nanocages. *Adv. Healthc. Mater.* **2023**, *12*, 2202932.
(59) Präbst, K.; Engelhardt, H.; Ringgeler, S.; Hübner, H. Basic Colorimetric Proliferation Assays: MTT, WST, and Resazurin. In *Cell Viability Assays. Methods in Molecular Biology*; Gilbert, D. F., Friedrich, O., Eds.; Humana Press, 2017; Vol. *1601*.
(60) Enomoto, T.; Tanuma, S.; Yamada, M. A. ATP Requirement for the Processes of DNA Replication in Isolated HeLa Cell Nuclei. *J. Biochem.* **1981**, *89*, 801−807.
(61) Majumdar, C.; Frankel, F. R. Biological Sciences: Role of ATP in DNA Replication. *Nature* **1973**, *243*, 33−36.
(62) Uhlmann, E.; Peyman, A. Antisense oligonucleotides: a new therapeutic principle. *Chem. Rev.* **1990**, *90*, 543−584.

https://doi.org/10.1021/jacs.3c04345
J. Am. Chem. Soc. 2023, 145, 22903−22912